Picosecond IR–UV pump–probe spectroscopic study of the dynamics of the vibrational relaxation of jet-cooled phenol. I. Intramolecular vibrational energy redistribution of the OH and CH stretching vibrations of bare phenol

Yuji Yamada, Takayuki Ebata,[a),b)] Masakazu Kayano, and Naohiko Mikami[b)]
Department of Chemistry, Graduate School of Science, Tohoku University, Sendai, 980-8578, Japan

(Received 30 October 2003; accepted 20 January 2004)

The intramolecular vibrational energy redistribution (IVR) of the OH stretching vibration of jet-cooled phenol-h_6 (C_6H_5OH) and phenol-d_5 (C_6D_5OH) in the electronic ground state has been investigated by picosecond time-resolved IR–UV pump–probe spectroscopy. The OH stretching vibration of phenol was excited with a picosecond IR laser pulse, and the subsequent temporal evolutions of the initially excited level and the redistributed ones due to the IVR were observed by multiphoton ionization detection with a picosecond UV pulse. The IVR lifetime for the OH stretch vibration of phenol-h_6 was determined to be 14 ps, while that of the OH stretch for phenol-d_5 was found to be 80 ps. This remarkable change of the IVR rate constant upon the dueteration of the CH groups strongly suggests that the ''doorway states'' for the IVR from the OH level would be the vibrational states involving the CH stretching modes. We also investigated the IVR rate of the CH stretching vibration for phenol-h_6. It was found that the IVR lifetime of the CH stretch is less than 5 ps. The fast IVR is described by the strong anharmonic resonance of the CH stretch with many other combinations or overtone bands. © *2004 American Institute of Physics.*
[DOI: 10.1063/1.1668640]

I. INTRODUCTION

The vibrational relaxation of the OH and CH stretching vibrations in the condensed phase has been extensively studied experimentally and theoretically.[1–14] For the OH stretching vibration, the importance of its dynamics is owing to the fact that most of the chemical reactions in protic solvent, such as water or alcohols, occur through the hydrogen (H) bonds among the OH groups and that absorption bands of the H-bonded OH stretching vibrations exhibit a characteristic spectral feature such as substantial frequency reduction and broadening,[15] which is quite different from the feature of other vibrations. The broadening involves the dephasing, the population decay, and the inhomogeneous broadening under different environments, which are often difficult to be discriminated from each other. In the condensed phase, the relaxations of the OH and CH stretching vibration have been studied by many workers for a long time. Particularly, it is known that the CH stretch vibrations of aliphatic alcohol exhibit a very fast population decay—i.e., a short T_1 relaxation lifetime.[9–11] The fast decay is interpreted by the strong coupling with the overtone band of the CH bending.

One of the key issues on the vibrational relaxation of such a high-frequency vibration is to find the state(s) to which the pumped level is strongly coupled. We call such a strongly coupled state a ''doorway state'' of the IVR.[16–19] As described above, in aliphatic alcohols the CH stretch is coupled strongly with overtones of the CH bending, and a similar circumstance may be seen in aromatic molecules. In this respect, it will be interesting to find the doorway state(s) for the IVR from the OH stretching vibration. In spite of its fundamental importance, the investigation is very difficult in the condensed phase because of the fact that the OH group is a quite sensitive functional group under the influence of solvents.[20,21]

Phenol is the simplest aromatic molecule having the OH group, and the electronic and vibrational states of the H-bonded clusters with solvent molecules have been extensively studied in a supersonic jet.[22–33] Recently, we have reported a picosecond IR–UV pump–probe spectroscopic study of the intramolecular and intracluster IVR of the OH stretching vibration of bare phenol and its dimer in their S_0 state.[34] We observed the population decay of the initially pumped level prepared by a picosecond IR light, as well as the generation of the redistributed levels. We found that the IVR lifetime of the OH stretch is 14 ps for bare phenol. In the dimer, the IVR lifetime of the H-donor OH stretch was substantially reduced, while that of the acceptor OH was almost unchanged. Though we have found a substantial change in the IVR lifetime of the OH stretch vibration, we have not yet made it clear how the high-frequency OH stretch energy is redistributed to the low-frequency bath modes or whether there exist some specific doorway states for the IVR of the OH stretch vibration.

In this paper, we present a more detailed study of the IVR of the OH stretch of bare phenol by examining its isotope effect, in which we compared the lifetime of the OH stretch of phenol with that of phenol-d_5 (C_6D_5OH). The purpose of this study is to examine whether the CH stretch-

[a)]Authors to whom correspondence should be addressed.
[b)]Electronic mail: ebata@qclhp.chem.tohoku.ac.jp

ing vibrations are involved in the doorway states that are thought to be coupled strongly to the OH stretching vibration. The possibility that the CH stretch vibrations act as effective bath modes of the OH stretch was recently suggested by Ishinchi *et al.*[35,36] in their study of the bandwidth measurement of the IR absorption spectrum, though there remains some ambiguity on the rotational contour analysis unless the individual lines are fully resolved.[37,38] An alternative method is to measure the IVR lifetime directly by picosecond IR–UV pump–probe spectroscopy, where we observe the time evolutions of the population of the IR-pumped OH level as well as those of the redistributed levels after the IVR. If the levels involving the CH stretches play the role of the doorway states, we will observe a large difference in the IVR lifetime of the OH stretch vibration by the deuterium substitution of the CH groups.

We also studied the IVR of the CH stretch vibrations of phenol. As was described above, the aliphatic CH stretch of alcohol exhibits fast T_1 relaxation in solution, which is explained by the strong ''CH-stretch–CH-bend'' coupling.[9–11] We investigate whether such a strong coupling also exists in the aromatic CH stretch under the collision-free condition in a supersonic jet. All the results presented in this work will provide us with a clear picture of the IVR mechanism of the high-frequency OH and CH stretching vibrations of phenol.

II. EXPERIMENT

A detailed description of the experimental setup of picosecond IR–UV pump–probe spectroscopy was given in our previous paper.[34] Briefly, a fundamental output (1.064 μm) of a mode-locked picosecond Nd^{3+}:YAG laser (Ekspra PL2143B) was split into two parts. The major one was frequency tripled and was introduced into an OPG/OPA system (Ekspra PG401SH) for a tunable UV light generation. Typical bandwidth and output power of the UV light was 10 cm^{-1} and 50–100 μJ, respectively. The minor part of the 1.064 μm output was introduced into a pair of $LiNbO_3$ crystals to generate tunable IR light pulses. The two crystals were separated by 1 m and were placed on rotational stages. Due to a severe phase matching condition between two angles, a bandwidth of IR light was achieved as narrow as 15 cm^{-1} and its typical output power was 50–100 μJ. CaF_2, ZnSe, and Ge plates were used so that only the signal light at $\sim$3 μm was introduced into a vacuum chamber as a pump pulse. As was described in the previous paper, the temporal shape of the pump or probe laser pulse was determined by fitting the time profile of the IR–UV pump–probe signal of the CH stretching vibration (mode 20) of benzene: because of that, the CH stretch of benzene does not exhibit an IVR and a sharp $6_0^1 20_1^1$ vibronic transition was observed.[33] The time profile of the $6_0^1 20_1^1$ band intensity was well fitted by assuming a Gaussian shape for both the two pulses having a pulse width of 14 ps.

Jet-cooled phenol-h_6 (or phenol-d_5) was generated by a supersonic expansion of phenol (or phenol-d_5) vapor seeded in He carrier gas (typically 3 atm) into vacuum through a pulsed nozzle (General valve) having a 0.8 mm aperture. The free jet was skimmed by a skimmer having a 0.8 mm diameter (Beam dynamics) located at 30 mm downstream of the nozzle. Phenol was heated up to 310 K to obtain a sufficient vapor pressure.

The IR and UV lasers were introduced into a vacuum chamber in a counterpropagated manner and crossed the supersonic beam at 50 mm downstream of the skimmer. The vibrationally excited molecules in the supersonic beam were ionized by $1+1$ resonance-enhanced multiphoton ionization (REMPI) via the S_1 state, and the ions were repelled to the direction perpendicular to the plane of the molecular and laser beams. The ions were then mass analyzed by a 50 cm time-of-flight tube and were detected by an electron multiplier (Murata Ceratron). The transient profiles of the pump–probe ion signals were observed by changing a delay time between UV and IR pulses with a computer-controlled optical delay line. The ion signals were integrated by a boxcar integrator (Par model 4420/4400) connected with a microcomputer.

We also measured the ionization-detected IR spectrum (IDIRS) of phenol by using a nanosecond laser system. The setup was described previously in our papers.[24–29] Briefly, the frequency of the UV laser was fixed to the origin band of the S_1-S_0 transition of phenol, and the ground-state population of phenol was monitored by $(1+1)$ REMPI with the UV light. Under this condition, a tunable IR light was introduced at $\sim$50 ns prior to the UV pulse. When the IR frequency was resonant to the vibrational transition, the ground-state population was depleted due to the vibrational excitation, leading to a depletion of the ion intensity. Thus the IR spectrum was obtained as an ion-dip spectrum by scanning the IR frequency while monitoring the phenol ion intensity. The spectral resolution of the IR light was 0.1 cm^{-1}.

Phenol-h_6 (99.0%) was purchased from Wako Chemicals Industry Ltd. and was purified by vacuum sublimation before use. Phenol-d_5 was prepared by adding a few drops of water to phenol-d_6 (98-atom %D) purchased from Sigma-Aldrich Fine Chemicals.

III. RESULTS

A. IR spectra of phenol-h_6 and phenol-d_5

Figure 1(a) shows the IR spectra of phenol-h_6 in the 2900–3700 cm^{-1} region. Two types of spectra are shown, which are obtained by different methods. The upper trace of Fig. 1(a) shows the ionization detected IR (IDIR) spectrum observed by the nanosecond laser system. The lower trace of Fig. 1(a) is the ion-gain IR spectrum observed by the picosecond laser system. Figure 1(b) shows the picosecond IR spectrum of phenol-d_5 in the OH stretch region. An excitation scheme of the ion-gain measurement is shown in the inset of Fig. 1. In the picosecond ion-gain spectrum, the UV laser frequency (ν_{UV}) was fixed at 35 650 cm^{-1}, which refers to the electronic transition ($v'-v''$ transition) from the vibrational levels (v'') generated by the IVR following vibrational excitation, and the UV pulse was introduced at a delay time (Δt) of 40 ps after the IR pulse excitation.

The spectral feature of the picosecond ion-gain IR spectra corresponds very well to the nanosecond IDIR spectrum

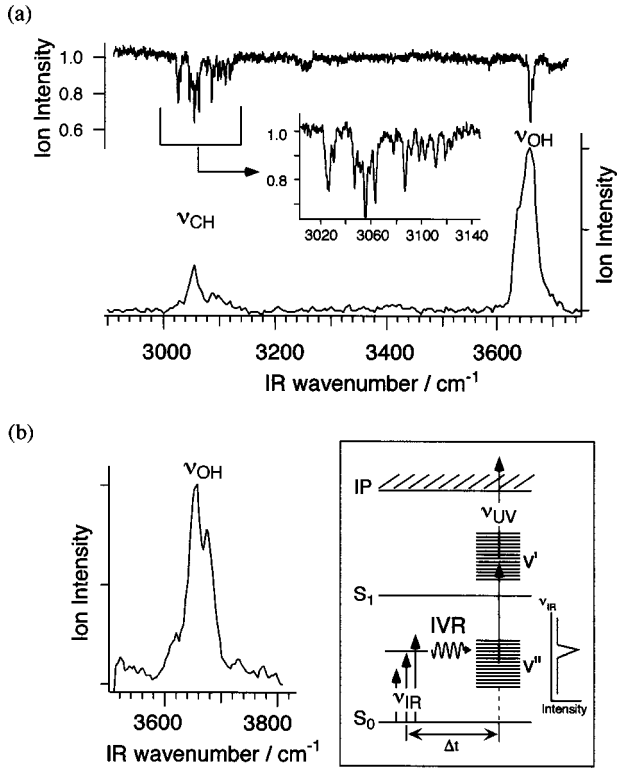

FIG. 1. (a) IR spectra of phenol-h_6 in a supersonic beam. The upper figure was obtained by monitoring the origin band while scanning the IR frequency with a nanosecond laser system. The lower is the ion-gain IR spectrum obtained with the picosecond laser system. The UV pulse was introduced at a delay time of 40 ps and its frequency was fixed at 35 650 cm^{-1}, corresponding to the transition from the redistributed levels. (b) Picosecond ion-gain IR spectrum of phenol-d_5 in the OH stretch region. The UV pulse with its frequency fixed at 35 970 cm^{-1} was introduced at a delay time of 350 ps. The inset shows the energy level diagram and the excitation scheme.

TABLE I. Observed bands in the CH stretching vibration region of the IR spectrum for phenol-h_6 [see Fig. 1(a)], compared to previous data.[a]

Observed position (cm^{-1}) (intensity[b])	Previous data[a] (cm^{-1})
3024 (m)	
3026 (s)	3027
3031 (m)	
3037 (w)	
3042 (w)	
3047 (s)	3049
3050 (m)	
3052 (m)	
3056 (s)	3063
3059 (m)	
3066 (w)	
3069 (w)	
3078 (m)	3070
3087 (s)	3087
3092 (m)	
3098 (m)	
3103 (m)	
3111 (m)	
3119 (m)	
3124 (w)	
3127 (w)	

[a]Bist *et al.* (Ref. 39).
[b]Intensity of bands: s=strong, m=medium, and w=weak.

(upper) except for the spectral resolution between them. In the phenol-h_6 spectra, the band at 3657 cm^{-1} is the OH stretching vibration and many bands appearing in the 3000–3140 cm^{-1} region are associated with the CH stretching vibrations. The inset of Fig. 1(a) shows an enlarged portion of the CH stretching region. At least 20 bands are identified in this region, which are as many as 4 times the number of CH oscillators of phenol. The observed bands are listed in Table I together with the values reported by Bist and co-workers.[39] Though they reported five bands in this region, the number of bands found in this work is much larger than that reported by them. It is not straightforward to make a definitive assignment for each band. Such a congested feature is thought to be due to the strong anharmonic resonance between the inherent CH stretch vibrations and isoenergetic levels associated with overtones and/or combinations. As seen later, the strong anharmonic resonance causes the fast IVR of the CH stretching vibrations.

In the picosecond ionization gain IR spectrum of the OH stretching vibration of phenol-d_5 shown in Fig. 1(b), the delay time (Δt) between the IR and UV light pulses was fixed to 350 ps, and the UV frequency ($\nu_{UV}=35\,970$ cm^{-1}) was tuned to the electronic $v'-v''$ transition from the redistributed vibrational levels. The precise frequency of the OH stretching vibration of phenol-d_5 was obtained to be 3657 cm^{-1} by IDIR spectroscopy with the nanosecond laser system. Thus the OH stretching vibrational frequency of phenol-d_5 is the same as that of phenol-h_6, and in the next section, we investigate the IVR dynamics.

B. IVR of the OH stretching vibration of phenol-h_6

Figure 2 shows the transient (1+1) REMPI spectra of phenol-h_6 measured at several delay times after exciting the OH stretching vibration at 3657 cm^{-1}. All the UV spectra are shown in the manner that the REMPI spectrum measured without introducing the IR laser pulse is subtracted. At short delay times, several sharp bands are seen in the lower-frequency region of the spectra and they rapidly diminish with delay time. Those bands are assigned to the ''hot'' transitions from the IR-pumped OH stretch level, such as the OH_1^0 band (32 690 cm^{-1}) and other vibronic bands. On the other hand, a very broad band appearing in the region higher than 34 000 cm^{-1} are assigned to the $v'-v''$ transitions from the vibrational levels (v'') generated by the IVR from the OH stretch level. Though the broad continuum is already seen even at a very short delay time, its intensity monotonically increases without showing any change in the spectral pattern. In addition, the time constant of the intensity rise shows a good correlation with the decay of the sharp bands.

Figure 3 shows the time profiles of the band intensities versus the delay time after the IR excitation of the OH stretching vibration obtained by monitoring the UV wave numbers given in the figure. The sharp band (a) at $\nu_{UV}=OH_1^0$ diminishes within 50 ps, while the intensity of the broad band increases to make a plateau after 50 ps. By con-

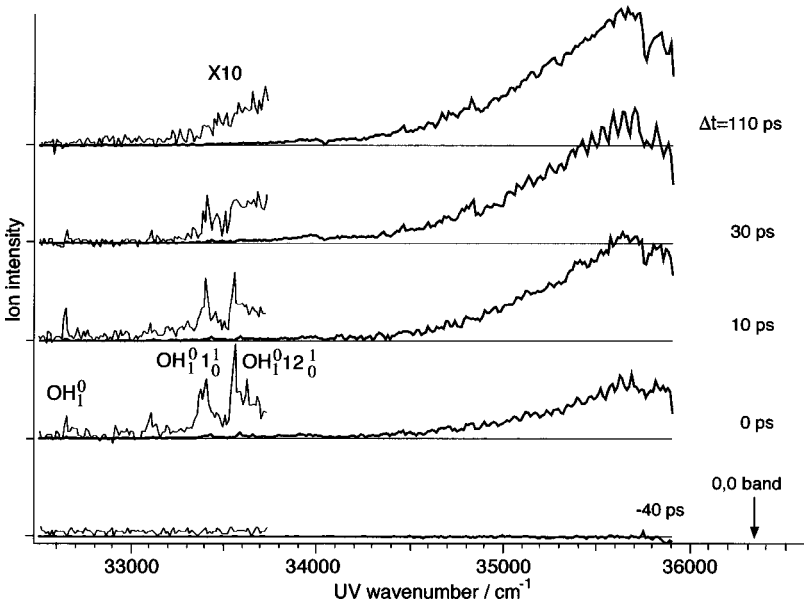

FIG. 2. Transient 1+1 REMPI spectra of phenol-h_6 obtained by scanning the UV frequencies at several delay times after pumping the OH stretching level.

voluting the time profiles with the laser pulse width of 14 ps, the decay profile of the OH_1^0 band can be fitted by a single-exponential decay curve

$$I(t) = I_0 \exp(-t/\tau_{\mathrm{IVR}}), \tag{1}$$

with the lifetime $\tau_{\mathrm{IVR}} = 14$ ps, corresponding to the rate constant of $k_{\mathrm{IVR}} = 7.1 \times 10^{10}\ \mathrm{s}^{-1}$. The convoluted curved is shown as a solid curve in Fig. 3(a). The profiles of the broad band can be also fitted by an exponential rising curve

$$I(t) = I_0\{1 - \exp(-t/\tau_{\mathrm{IVR}})\}, \tag{2}$$

with the same time constant $\tau_{\mathrm{IVR}} = 14$ ps. The convoluted time profiles obtained with the excitation at various probe wavelengths are also shown in Figs. 3(b)–3(d) with solid curves. Although the IVR lifetime was accidentally the same with the laser pulse width, the agreement between the two convoluted curves above indicates the obtained lifetime to be unambiguous. It should be noted that the time profiles of the broad band were independent of the monitoring UV wavelength, which will be discussed later. Thus the IVR lifetime of the OH stretch in bare phenol-h_6 is determined to be 14 ps.

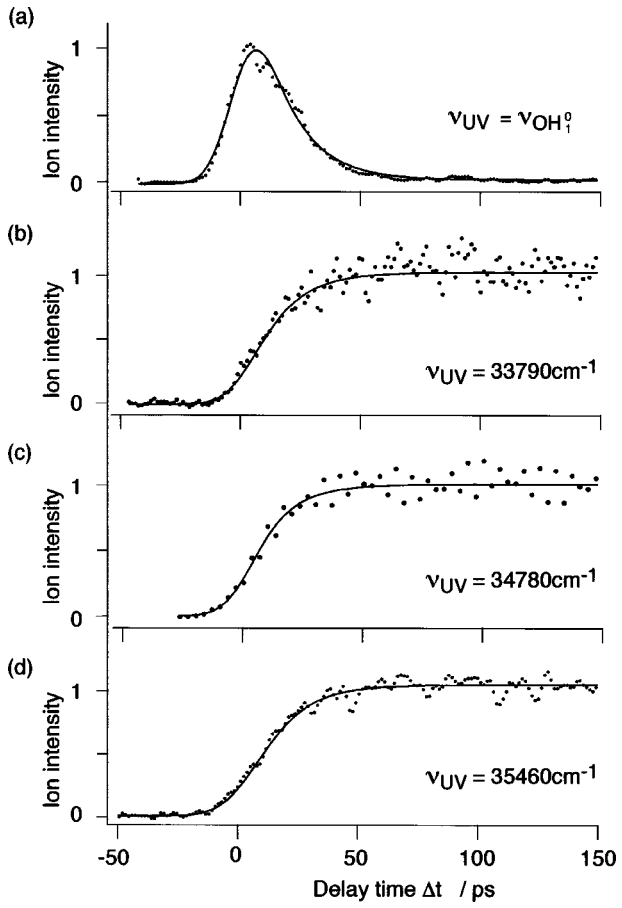

FIG. 3. (a) Transient time profile of OH_1^0 band of phenol-h_6. (b), (c), (d) Time profiles of the IVR-redistributed levels of phenol-h_6 obtained at different probe frequencies (33 790, 34 790, and 35 460 cm^{-1}). The solid curves were convoluted ones by setting (a) $\tau_{\mathrm{decay}} = 14$ ps and (b), (c), (d) $\tau_{\mathrm{rise}} = 14$ ps. The undulation of the plateaus is due to the instability of the laser system.

C. IVR of the CH stretching vibration of phenol-h_6

As shown in Fig. 1(a), the IR spectrum of the CH stretching vibrations of phenol-h_6 exhibits a complicated feature consisting of many bands caused by the strong anharmonic resonance. Among these bands appearing, we examined the IVR of a band centered at 3056 cm^{-1} because of its intensity. As seen in the IDIR spectrum [the upper spectrum of Fig. 1(a)], three peaks are clearly identified: an intense peak at 3056 cm^{-1} and two satellite peaks at 3047 and 3063 cm^{-1}, which cannot be resolved in the lower spectrum of Fig. 1(a). Thus these bands are thought to be simultaneously excited when the frequency of the picosecond IR pulse is tuned to 3056 cm^{-1}.

We first measured the transient UV spectrum after the IR pump of the CH stretch vibration. The observed transient UV spectra were much weaker than the case of the OH stretch because of the weaker IR absorption intensity of the CH vibration than that of the OH stretch vibration. Nevertheless,

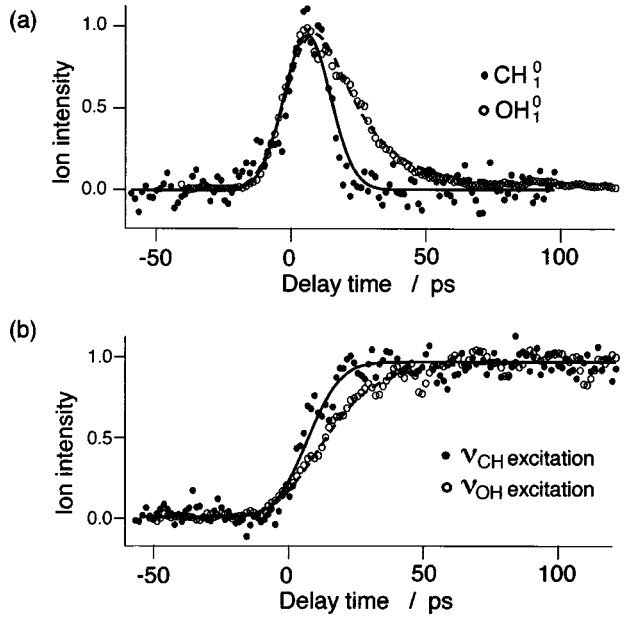

FIG. 4. (a), (b) Time profiles of the CH_1^0 band and IVR-redistributed levels after exciting the CH stretching vibrations of phenol-h_6 (●). Also shown are the results of the IVR of the OH stretching vibration (○). The solid curves are the convoluted curve by assuming an IVR lifetime of 5 ps.

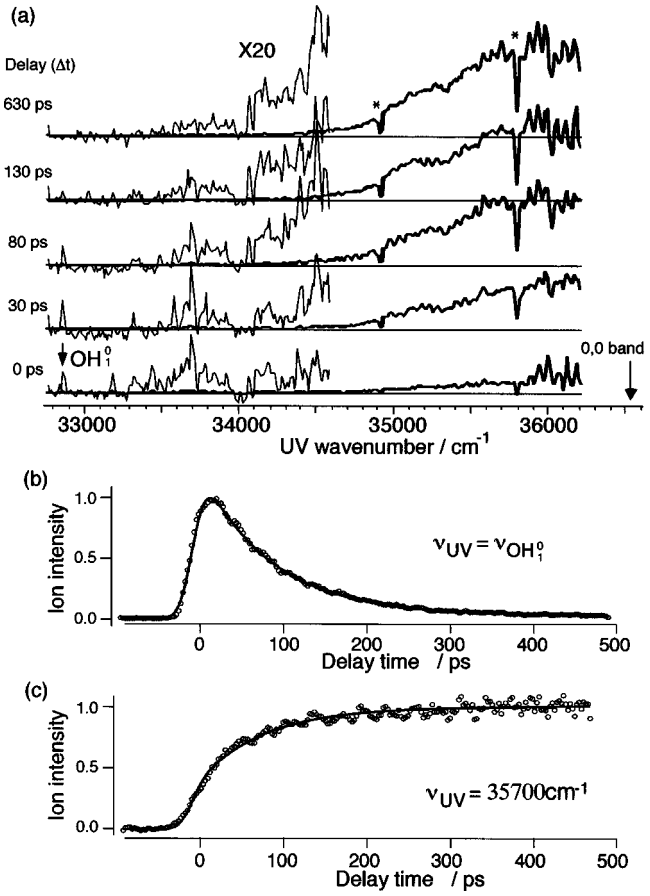

FIG. 5. (a) Transient $1+1$ REMPI spectra of phenol-d_5 obtained by scanning the UV frequencies at several delay times after pumping the OH stretching level. Asterisks mean a signal loss due to weak power outputs at particular UV wavelengths in our laser system. (b), (c) Time profiles of the OH_1^0 band and the broad band derived from the IVR redistributed levels after exciting the OH stretching vibration of phenol-d_5. Convoluted curves by setting the IVR lifetime of the OH level as 80 ps are also shown.

we could see that the observed spectrum exhibits a very similar feature to the case of the OH stretching excitation—that is, a fast decay of the CH_1^0 transition—and the corresponding rapid rise of the broad continuum at the higher-UV-frequency region. Figure 4 shows the time profiles of the pump–probe signal intensity versus the delay time after the IR excitation of the CH band at 3056 cm^{-1}. Figure 4(a) represents the time profile of the CH_1^0 band at 33 300 cm^{-1}, and Fig. 4(b) shows that of the broad band at 35 650 cm^{-1} which are due to the transition from the redistributed levels. For comparison, the time profiles observed in the OH stretch excitation are reproduced by open circles, indicating that the decay of the CH_1^0 band is substantially faster than that of the OH_1^0 band. In accordance with the fast decay of the CH_1^0 band, the intensity of the broad band from the redistributed levels shows a faster rise than the case of the OH excitation. By convoluting the time profiles of the CH_1^0 band and the redistributed levels with the 14 ps pump–probe laser pulse width, we estimated that the IVR lifetime of the CH stretch vibration is less than 5 ps, which is the shortest lifetime determined accurately with our laser system. Thus we conclude that the IVR of the CH stretching vibration at 3056 cm^{-1} occurs over 3 times faster than that of the OH stretching vibration, in spite of the fact that the frequency of the former vibration is about 600 cm^{-1} lower than the latter.

D. IVR of the OH stretching vibration of phenol-d_5

As was described in the Introduction, the IVR measurement of phenol-d_5 having no CH oscillators is effective for the evaluation of the contribution of the CH stretch vibrations as the bath mode for the IVR of the OH stretch. Figure 5(a) shows the transient $(1+1)$ REMPI spectra observed at several delay times after the OH band excitation of phenol-d_5. Similarly to phenol-h_6 (Fig. 2), several sharp vibronic bands due to resonance transitions from the OH stretching level are clearly seen in the lower-frequency region at short delay times. Interestingly, their decay is substantially slower than those of phenol-h_6; the OH_1^0 band, for example, is clearly seen even at a delay time of 130 ps.

We then observed the time evolutions of the transient $(1+1)$ REMPI signal intensity as a function of the delay time by fixing the UV laser frequency to several bands in the UV spectrum. Figures 5(b) and 5(c) show the time profiles of the sharp OH_1^0 band at 32 870 cm^{-1} and the broad band at 35 700 cm^{-1}, respectively. As seen in Fig. 5(b), the OH_1^0 band decays exponentially with the lifetime $\tau_{IVR}=80$ ps. Accordingly, in Fig. 5(c), the time profile of the broad band intensity exhibits a rise with the same time constant (80 ps). Therefore, the IVR lifetime of the OH stretching vibration of bare phenol-d_5 is determined to be 80 ps ($k_{IVR}=1.3\times10^{10}$ s^{-1}), which is 5.7 times slower than that of phenol-h_6 (14 ps). Thus we found that the deuteration of the CH groups dramatically decelerates the IVR rate of the OH stretching vibration. It should be also noted that the time profiles of the rise of the broad bands were the same at different monitoring UV frequencies, similar to the case of phenol-h_6.

TABLE II. Calculated vibrational frequencies (in cm^{-1}) of all modes in phenol-h_6 and phenol-d_5 by the B3LYP/cc-pVTZ level, compared to the experimental ones.

			Phenol-h_6		Phenol-d_5	
Symmetry		Mode	Calc.[b]	Expt.[d]	Calc.[c]	Expt.[d]
a'	18b	X-sensitive	393	403	379	386
	6a	X-sensitive	520	526	510	513
	6b	ring	614	619	592	595
	12	X-sensitive	803	823	747	754
	1	ring	985	999	807	811
	18a	CH bend	1012	1025	826	831
	15	CH bend	1060	1070	834	840
	9b	CH bend	1139	1150	865	879
	9a	CH bend	1154	1168	950	960
		OH bend	1155	1176	1011	1021
	7a	CO stretch	1243	1261	1168	1179
	3	CH bend	1304	1277	1191	1187
	14	CC stretch	1331	1343	1305	1300
	19b	CC stretch	1457	1472	1363	1372
	19a	CC stretch	1484	1501	1395	1405
	8a	CC stretch	1585	1603	1563	1572
	8b	CC stretch	1595	1610	1576	1578
	13	CH stretch	3045	3027	2261	2262
	7b	CH stretch	3063	3049	2273	2283
	2	CH stretch	3071	3063	2284	2295
	20b	CH stretch	3085	3070	2296	2302
	20a	CH stretch	3091	3087	2304	2313
		OH stretch	3690	3656	3712	3656
a''	11	X-sensitive	224	244	212	232
		OH torsion	344	309	343	307
	16a	CC twist	410	409	361	357
	16b	X-sensitive	501	503	429	431
	4	CC twist	683	686	548	550
	10b	CH bend	744	751	619	625
	10a	CH bend	801	817	630	694
	17b	CH bend	870	881	751	766
	17a	CH bend	940	973	767	720
	5	CH bend	960	995	802	825

[a]Regarding molecular symmetry of phenol as not C_{2v} but C_s.
[b]Scaled with factor of 0.9666 in order to give the least-squares deviation to the experimental data of phenol-h_6.
[c]Scaled with factor of 0.9725 in order to give the least-squares deviation to the experimental data of phenol-d_5.
[d]Bist *et al.* (Ref. 39).

IV. DISCUSSION

A. "Doorway states" and IVR mechanism of the OH stretching vibration of phenol

The substantial isotopic effect on the IVR rate constant of the OH stretch vibration of phenol-d_5 and phenol-h_6 strongly indicates that the anharmonic couplings between the OH stretch and isoenergetic vibrational levels are quite different in these two isotopomers. We first assume that the IVR rate (k_{IVR}) is expressed by the Fermi's golden rule equation[40]

$$k_{\mathrm{IVR}}=\frac{2\pi}{\hbar}|V_{\mathrm{inh}}|^2\rho(\nu_{\mathrm{OH}}), \tag{3}$$

where V_{anh} is the averaged anharmonic coupling matrix element between the OH stretch level and bath modes, and $\rho(\nu_{\mathrm{OH}})$ is the state density of the bath modes at the energy of the OH stretching vibration. We calculated the state density at 3657 cm^{-1} for phenol-h_6 and -d_5 by the direct counting method under a harmonic oscillator approximation with fundamental frequencies of the vibrations taken from the experimental data[39] reported by Bist *et al.*, which are listed in Table II. As mentioned above, however, because of the congested CH stretch bands in the IR spectrum, it was difficult to find a reliable assignment of their vibrational modes for the state density calculation. In order to solve this problem, we calculated vibrational frequencies for the optimized geometry of phenol and compared them with those given by Bist *et al.* A density functional theory (DFT) calculation using the GAUSSIAN 98 suite of programs[41] with the B3LYP/cc-pVTZ level was employed and the calculated frequencies are also listed in Table II. As seen in the table, the agreement between the reported and calculated frequencies is acceptable for the state density calculation. By using these assigned frequencies, we calculated the state densities for both isotopomers and obtained the densities of states having a' species with C_s molecular symmetry at 3657 cm^{-1} to be 110 and 350 states/cm^{-1} for phenol-h_6 and phenol-d_5, respectively.

If we assume that the uniform anharmonic coupling matrix elements with all the bath modes[42]—that is, V_{anh} in Eq. (3)—are the same between two isotopomers, the IVR rate of

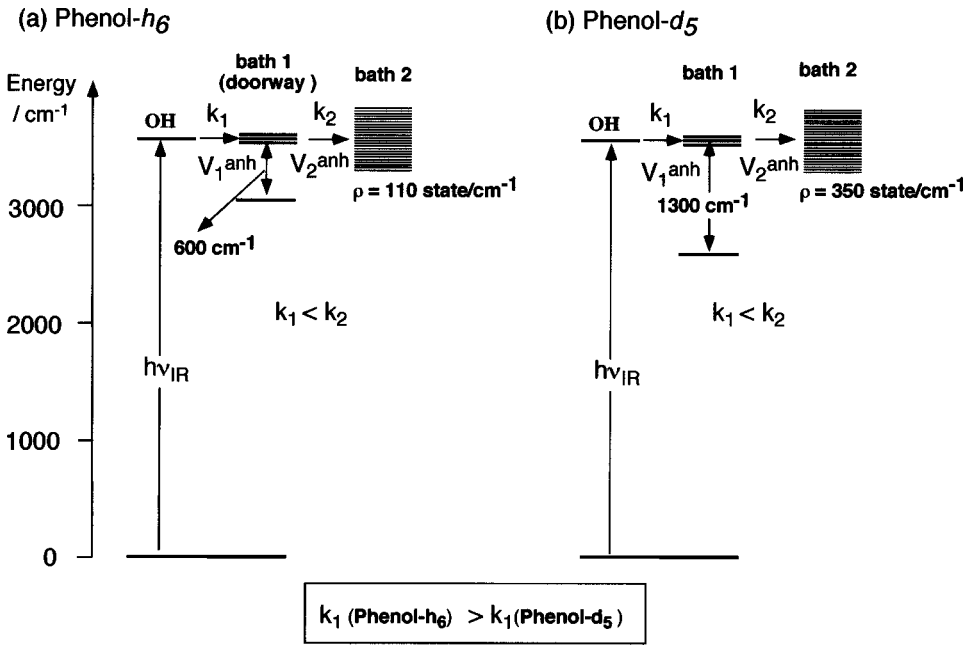

FIG. 6. Coupling scheme between the OH stretch level and "bath 1 and bath 2" of (a) phenol-h_6 and (b) phenol-d_5. Here V_1^{anh} and V_2^{anh} are the anharmonic coupling matrix elements between the OH stretch and bath 1, and bath 1 and bath 2, respectively. k_1 and k_2 are the IVR rate constants from the OH stretch to bath 1, and from bath 1 to bath 2, respectively.

phenol-d_5 would be about 3 times larger than phenol-h_6, from the difference in the state density. The observed results are opposite to such an expectation, and it is concluded that the anharmonic coupling between the OH stretch and bath modes is much stronger in phenol-h_6 than in phenol-d_5. How do we explain the large difference of the anharmonic coupling for two molecules? First, it is unlikely that the anharmonic couplings between the OH stretch and all bath modes are uniformly decreased by changing CH to CD. So it is more reasonable to consider that only a limited number of levels in the bath modes are strongly coupled to the OH stretch level, which are largely affected by the deuterium substitution of the CH group.

On the basis of the above result, we have examined a hierarchical model of the bath modes for the IVR mechanism of the OH stretching vibration, as shown in Fig. 6. The OH stretching vibration is preferentially coupled to the "bath 1," which we call "doorway states," with the low-order coupling. This coupling is symbolically represented by V_1^{anh}, and k_1 means the IVR rate constant from the OH stretch level to the "doorway states." The "doorway states" are further coupled to another vibrational levels of high density—i.e., "bath 2." This coupling V_2^{anh} results in k_2 for IVR from "bath 1" to "bath 2." In this model, the time evolutions of each state population are expressed as

$$I_{\text{OH}}(t) = I_0 \exp(-k_1 t), \tag{4}$$

$$I_{\text{bath 1}}(t) = \frac{k_1}{k_2 - k_1} I_0 \{\exp(-k_1 t) - \exp(-k_2 t)\}, \tag{5}$$

and

$$I_{\text{bath 2}}(t) = I_0 \left[1 - \exp(-k_1 t) - \frac{k_1}{k_2 - k_1} \times \{\exp(-k_1 t) - \exp(-k_2 t)\} \right]. \tag{6}$$

In this model, the rate constant (k_{IVR}) obtained from the decay of the OH_1^0 band corresponds to k_1 in Fig. 6(a). Similarly, the observed rise curve of the broad band will be a superposition of $I_{\text{bath 1}}(t)$ and $I_{\text{bath 2}}(t)$ according to the Franck–Condon factor of the $v' - v''$ transitions from these states. As mentioned above, however, the observed rise curves of the broad band derived from redistributed levels was well fitted by Eq. (2), and the obtained rate constant was the same as k_1, being irrespective of the monitoring UV wavelength for both phenol-h_6 and -d_5. If k_2 is comparable to or smaller than k_1, the time constant of the rise of the broad band will be much smaller than the decay rate of the OH_1^0 band, and the rise curves will depend on the monitoring UV wavelength owing to a variation of the ratio between the $v' - v''$ transition intensities from "bath 1" and "bath 2." Thus this result means that k_2 is much larger than k_1 in both isotopomer cases. Actually, when $k_1 \ll k_2$, Eq. (6) becomes

$$I_{\text{bath 2}}(t) \approx I_0 [1 - \exp(-k_1 t)], \tag{7}$$

which is equal to Eq. (2). The condition $k_1 \ll k_2$ is also confirmed by the fact that we did not see any change of spectral pattern in the broad continuum as mentioned previously. As seen in Eq. (5), when $k_1 \ll k_2$, the intensity of $I_{\text{bath 1}}$ becomes very small so that the transition from bath 1 will be buried by the continuum transition from bath 2. Therefore, we conclude k_2 is much larger than k_1 and the "OH stretch $\rightarrow$doorway sate" energy flow is the rate-determining step in the whole IVR process of the OH stretching vibration in both isotopomers.

Next, we will discuss which vibrational mode(s) is forming the "bath 1"—that is, doorway sate. We can safely assume that V_1^{anh} involves a low order of the anharmonic coupling, and it is thought that the doorway states consist of rather high-frequency modes such as the CH(CD) stretching vibration. The assumption that "bath 1" consists of CH(CD) stretches can explain reasonably the isotopic effect on the

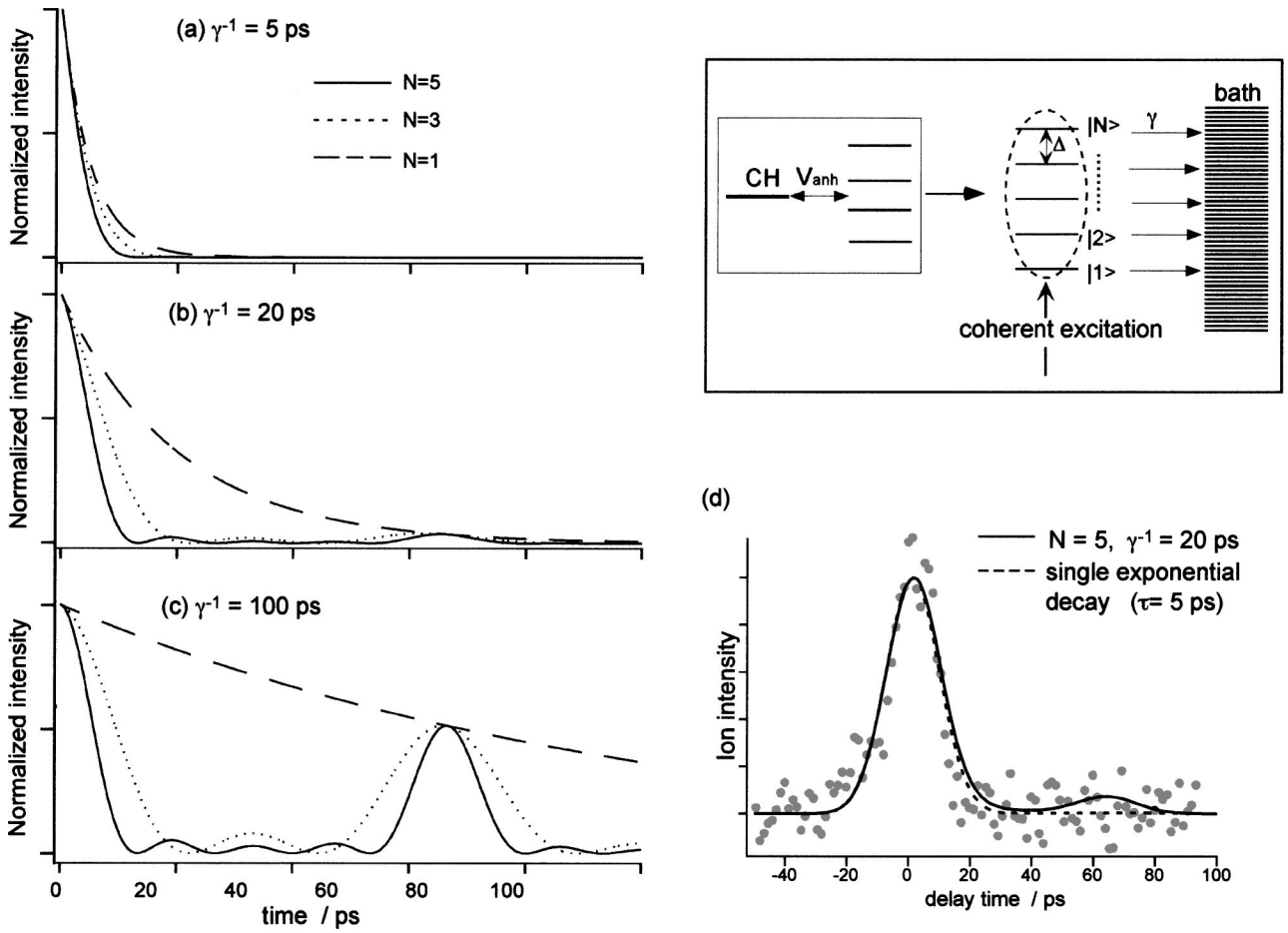

FIG. 7. (a)–(c) Calculated time profile of the CH levels after coherent excitation of the three-level system ($N=3$, dotted curve) and five-level system ($N=5$, solid curves). Also shown is the decay curve with $N=1$. In the inset is shown the coupling scheme, where Δ is the interval between the each level and γ^{-1} is the lifetime due to the IVR toward dense bath modes. (d) Comparison between the observed time profile of the CH_1^0 band (solid circles) and the convoluted curve by assuming $N=5$ and $\gamma^{-1}=20$ ps (solid curve) with a laser pulse width of 14 ps. Also shown is the convoluted decay curve by assuming $N=1$ and $\gamma^{-1}=5$ ps (dashed curve).

IVR rate of the OH stretch. There is a large difference in energy between the ''OH–CH stretches'' (550–650 cm^{-1}) and the ''OH–CD stretches'' (1350–1450 cm^{-1}). So the latter may require a larger quantum number of a vibration for energy conservation than the former. Thus, by considering the propensity rule[43] that the anharmonic coupling between states with smaller quantum number change should be larger, we can conclude that V_1^{anh} of phenol-h_6 is larger than that of phenol-d_5. This large change of the rate-determining step of the IVR from the OH stretch level results in a smaller IVR rate constant of the OH stretch of phenol-d_5 than that of phenol-h_6, as was observed experimentally.

Further evidence for the doorway state can be obtained by investigating IVR of phenol-d_1—that is, phenol-OD. However, the measurement of phenol-d_1 is unsuccessful at present because of the insufficient IR laser power in the OD stretching region, and we are now making further efforts.

B. Fast IVR of the CH stretching vibrations and the effect of anharmonic resonance

Though the CH stretching frequency is about 600 cm^{-1} smaller than that of the OH stretching vibration, we have found that the IVR rate of the CH stretching vibration is 3 times faster than that of the OH stretching vibration. This faster IVR process of the CH stretching vibration can be explained by quantum interference due to coherent excitation of several states in the CH stretching vibrational region. As described above, more than 20 bands appear in this region of phenol, owing to the strong anharmonic resonance with the overtone and/or combination bands. Thus the picosecond IR laser pulse tuned at 3056 cm^{-1} coherently excites more than three levels, which may exhibit fast quantum interference. Furthermore, these levels are further coupled to the dense bath mode similar to the case of the OH stretching vibration, so that the population of these coherently excited sates may rapidly decay into the dense bath mode. The reason why we could not observe a quantum beat is due to the fact that the laser pulse used in the present work was not short enough to resolve it or the decay rate toward the dense manifold is faster than the recurrence time scale.

To confirm the possibility mentioned above, we simulated the time evolution of the multilevel system involving the CH stretch level, after their coherent excitations. The coupling scheme is shown in the inset of Fig. 7. Here we consider the zero-order CH level and two levels ($N=3$) or four levels ($N=5$), which are coupled via the interaction

matrix element V_{anh}, so that all levels become optically allowed. We assumed that the levels are equally spaced with an interval of $\Delta = 0.5\ cm^{-1}$ and that the equal coefficient of the CH stretch level is distributed in all levels. In addition, each level has an intrinsic width (γ) due to further IVR toward the dense bath modes. The calculation was carried for three γ values—that is, $\gamma = 1.1$, 0.27, and $0.053\ cm^{-1}$, which correspond to the lifetime of 5, 20, and 100 ps, respectively. As seen in the figure, the CH component decays faster than γ^{-1} (decay curve with $N=1$) due to the interference effect, and the decay becomes faster with an increase of N. Furthermore, it is seen that the simulation with a small value of γ—that is, $\gamma = 0.053\ cm^{-1}$—does not reproduce the observed fast decay. Thus the intrinsic lifetime must be short for the fast IVR of the CH level to be reproduced. Figure 7(d) shows a comparison of the observed decay with the calculated one for the five-level system and $\gamma^{-1} = 20$ ps, where good agreement is obtained. Thus the intrinsic (IVR) lifetime of each level is roughly estimated to be less than 20 ps.

The fast IVR rate constant of the aromatic CH stretching vibration shows a similarity with the well-known short T_1 relaxation lifetime of the CH stretching vibration observed for aliphatic alcohols in the condensed phase, which is interpreted by the strong coupling with the overtone band of the CH bending vibration.[11,12] The frequencies of the aliphatic CH stretches are 2800–2900 cm^{-1} and those of the CH bends are 1400–1500 cm^{-1}. Thus a strong anharmonic resonance between the CH stretches and the first overtone of the CH bends is expected, and this coupling has been thought to be the origin of the fast T_1 relaxation of the CH stretching vibrations. In the case of the aromatic CH stretch, however, the situation may not be similar. As seen in Table II, the aromatic CH stretching frequencies are 3000–3100 cm^{-1} and those of CH bend are 1000–1200 cm^{-1}, so that there is a large energy mismatch between the CH stretch and first overtone of the CH bend. Thus the candidates of the anharmonic resonance observed in the CH stretch vibrations seem to be not the first overtone of the CH bends, but other combination bands.

In order to examine which combination bands exist in the CH stretching vibration region, we have listed the overtone and combination bands restricted to two vibrational quanta by using the reported frequencies listed in Table II. Only four combination bands were found in the 3000–3150 cm^{-1} region—that is, mode $19b+8a$ ($=3075\ cm^{-1}$), $19b+8b$ ($=3082\ cm^{-1}$), $19a+8a$ ($=3104\ cm^{-1}$), and $19a+8b$ ($=3111\ cm^{-1}$). Surprisingly, all of these modes were the CC stretching vibration, but no levels involving the CH bending mode were listed in the two-quantum case. In expanding the limit of the quantum number restriction up to 3, we obtained more than 100 candidates, where half of them involved the CH bending mode. However, we cannot accurately determine which combination bands are strongly coupled to the CH stretching vibration because of a large number of candidates and the uncertainty of anharmonicity.

Such a strong anharmonic resonance of the CH stretch vibrations is also seen in other aromatic molecules, such as benzene,[44,45] toluene,[45] aniline,[46] and so on. In the IR spectra of toluene and aniline, more than 11 bands appeared in the CH stretch region. In benzene, mode 20 forms a Fermi tetrad in the 3000–3100 cm^{-1} region with the combination bands involving modes 1, 3, 6, 8, 15, and 19, where most of them are not the CH bending vibrations.[44] Thus we may conclude that the CH stretching vibrations are not necessarily coupled with CH bending, but are strongly coupled with the CC stretching vibrations in the case of the phenol molecule too. Then, we can predict that the strong anharmonic resonance is the common feature for the CH stretching vibration of aromatic molecules, which will cause the very fast vibrational relaxation of the CH stretching vibration even under isolated condition.

V. CONCLUSIONS

In this article, the IVR mechanism of the OH and CH stretching vibration of phenol in the S_0 state has been examined by picosecond time-resolved IR–UV pump–probe spectroscopy. The IVR lifetimes of the OH (14 ps for phenol-h_6 and 80 ps for phenol-d_5) and the CH ($\leqslant$ 5 ps) stretching vibrations have been directly obtained. The very fast IVR rate of the CH stretching vibrations is described by a strong anharmonic resonance with the other modes. For the IVR of the OH stretch, we found a remarkable isotope effect: that is, the IVR rate of phenol-h_6 is 5.7 times faster than that of phenol-d_5. The result represents strong evidence that the IVR of the OH stretching vibration occurs through the doorway states composed of the CH stretching vibrations. The present results suggest that the CH stretching vibrations will play also important role in the IVR of the OH stretch in other aromatic systems.

Further evidence of the role of the doorway state for the CH stretching vibration can be obtained by the examining the OD stretching vibration, such as phenol-d_1 (C_6H_5OD) and phenol-d_6 (C_6D_5OD), which is the future study.

ACKNOWLEDGMENTS

The authors would like to acknowledge Dr. A. Fujii, Dr. H. Ishikawa, and Dr. T. Maeyama for helpful discussions. This work is supported by a Grant-in-Aid for Scientific Research (Grant No. 1535002) by J.S.P.S.

[1] S. Woutersen, U. Emmerichs, Han-Kwang Nienhuys, and H. J. Bakker, Phys. Rev. Lett. **81**, 1106 (1998).
[2] A. J. Lock, S. Woutersen, and H. J. Bakker, J. Phys. Chem. A **105**, 1238 (2001); A. J. Lock and H. J. Bakker, J. Chem. Phys. **117**, 1708 (2002).
[3] M. F. Kropman and H. J. Bakker, Chem. Phys. Lett. **370**, 741 (2003).
[4] J. C. Deàk, S. T. Rhea, L. K. Iwaki, and D. D. Dlott, J. Phys. Chem. A **104**, 4866 (2000).
[5] M. S. Bergen and S. A. Rice, J. Chem. Phys. **77**, 583 (1982).
[6] A. C. Belch and S. A. Rice, J. Chem. Phys. **78**, 4817 (1983); G. Nielson and S. A. Rice, *ibid.* **78**, 4824 (1983).
[7] H. Graener and G. Seifert, J. Chem. Phys. **98**, 36 (1993).
[8] R. Rey and J. T. Hynes, J. Chem. Phys. **104**, 2356 (1996).
[9] A. Fendt, S. F. Fischer, and W. Kaiser, Chem. Phys. **57**, 55 (1981).
[10] L. K. Iwaki and D. D. Dlott, J. Phys. Chem. A **104**, 9101 (2000); D. D. Dlott, Chem. Phys. **266**, 149 (2001).
[11] R. Laenen and C. Rauscher, Chem. Phys. Lett. **274**, 63 (1997); R. Laenen, C. Rauscher, and A. Laubereau, *ibid.* **283**, 7 (1998).
[12] R. Laenen, C. Rauscher, and K. Simeonidis, J. Chem. Phys. **110**, 5814 (1999).
[13] E. J. Heilweil, M. P. Casassa, R. R. Cavanagh, and J. C. Stephenson, J. Chem. Phys. **85**, 5004 (1986).

[14] A. Staib, J. Chem. Phys. **108**, 4554 (1998).
[15] P. Schuster, G. Zundel, and C. Sandorfy, *Recent Developments in Theory and Experiments*, Vol. 2 of The Hydrogen Bond (North-Holland, Amsterdam, 1976).
[16] A. Mcllroy and D. J. Nesbitt, J. Chem. Phys. **92**, 2229 (1990).
[17] S. Cupp, C. Y. Lee, D. McWhorter, and B. H. Pate, J. Chem. Phys. **109**, 4302 (1998).
[18] D. F. Heller and S. Mukamel, J. Chem. Phys. **70**, 463 (1979).
[19] J. S. Hutchinson, W. P. Reinhardt, and J. T. Hynes, J. Chem. Phys. **79**, 4247 (1983).
[20] A. V. Iogansen, Spectrochim. Acta, Part A **55**, 1585 (1999).
[21] M. Rozenberg, A. Leowenschuss, and Y. Marcus, Phys. Chem. Chem. Phys. **2**, 2699 (2000).
[22] R. Lipert and S. D. Colson, J. Phys. Chem. **93**, 135 (1989).
[23] G. V. Hartland, B. F. Henson, V. A. Venturo, and P. M. Felker, J. Phys. Chem. **96**, 1164 (1992).
[24] S. Tanabe, T. Ebata, M. Fujii, and N. Mikami, Chem. Phys. Lett. **215**, 347 (1993).
[25] T. Ebata, T. Watanabe, and N. Mikami, J. Phys. Chem. **99**, 5761 (1995).
[26] A. Iwasaki, A. Fujii, T. Ebata, T. Watanabe, and N. Mikami, J. Phys. Chem. **100**, 16053 (1996).
[27] T. Watanabe, T. Ebata, S. Tanabe, and N. Mikami, J. Chem. Phys. **105**, 408 (1996).
[28] G. N. Patwari, T. Ebata, and N. Mikami, J. Chem. Phys. **116**, 6056 (2002).
[29] A. Fujii, T. Ebata, and N. Mikami, J. Phys. Chem. A **106**, 10124 (2002).
[30] G. A. Pino, C. Dedonder-Lardeux, G. Grégoire, C. Jouvet, S. Martrenchard, and D. Solgadi, J. Chem. Phys. **111**, 10747 (1999).
[31] M. Schmitt, J. Küpper, D. Spangenberg, and A. Westphal, Chem. Phys. **254**, 349 (2000).
[32] R. M. Helm and H. J. Neusser, Chem. Phys. **239**, 33 (1998).
[33] T. Ebata, A. Iwasaki, and N. Mikami, J. Phys. Chem. A **104**, 7974 (2000).
[34] T. Ebata, M. Kayano, S. Sato, and N. Mikami, J. Phys. Chem. A **105**, 8623 (2001).
[35] S. Ishiuchi, H. Shitomi, K. Takazawa, and M. Fujii, Chem. Phys. Lett. **283**, 243 (1998).
[36] S. Ishiuchi and M. Fujii, AIP Conf. Proc. **454**, 137 (1998).
[37] G. A. Bethardy and D. S. Perry, J. Chem. Phys. **98**, 6651 (1993).
[38] G. T. Fraser, B. H. Pate, G. A. Bethardy, and D. S. Perry, Chem. Phys. **175**, 223 (1993).
[39] H. D. Bist, J. C. D. Brand, and D. R. Williams, J. Mol. Spectrosc. **24**, 402 (1967).
[40] G. C. Schuatz and M. A. Ranter, *Quantum Mechanics in Chemistry* (Prentice Hall, Englewood Cliffs, NJ, 1993).
[41] M. J. Frisch *et al.*, computer code GAUSSIAN 98, revision A.7, Gaussian, Inc., Pittsburgh, PA, 1998.
[42] M. Bixon and J. Jortner, J. Chem. Phys. **48**, 715 (1968); **50**, 3284 (1969).
[43] J. T. Yardly, *Introduction to Molecular Energy Transfer* (Academic, New York, 1980).
[44] R. H. Page, Y. R. Shen, and Y. T. Lee, J. Chem. Phys. **88**, 5362 (1988).
[45] C. Minejima, T. Ebata, and N. Mikami, Phys. Chem. Chem. Phys. **4**, 1537 (2002).
[46] G. N. Patwari, T. Ebata, and N. Mikami, Chem. Phys. Lett. **361**, 453 (2002).